

Electrical and Thermal Transport of Layered Bismuth-chalcogenide EuBiS_2F at temperatures between 300 and 623 K

Yosuke Goto^{1,†}, Joe Kajitani², Yoshikazu Mizuguchi², Yoichi Kamihara¹, and Masanori Matoba^{1,*}

¹*Department of Applied Physics and Physico-Informatics, Faculty of Science and Technology, Keio University, Yokohama 223-8522, Japan*

²*Department of Electrical and Electronic Engineering, Tokyo Metropolitan University, Hachioji 192-0397, Japan*

We demonstrate the electrical and thermal transport of layered bismuth-based sulfide EuBiS_2F from 300 to 623 K. Although significant hybridization between Eu $4f$ and Bi $6p$ electrons was reported previously, the carrier transport of the compound is similar to those of F-doped LaBiS_2O , at least above 300 K. The lattice thermal conductivity is lower than that of isostructural SrBiS_2F , which is attributed to heavier atomic mass of Eu ions.

Bismuth-based chalcogenides/oxides have generated interest because of their functionality for thermoelectricity,¹⁾ superconductivity,²⁾ photocatalysis,³⁾ multiferroicity,⁴⁾ etc. Searching for novel thermoelectric materials is most fundamental issues for the development of thermoelectrics because maximum conversion efficiency of a thermoelectric device is primarily determined by material's dimensionless figure of merit, $ZT = S^2T\rho^{-1}\kappa^{-1}$, where T , S , ρ , and κ denote the temperature, Seebeck coefficient, electrical resistivity, and thermal conductivity, respectively.⁵⁾ Bismuth telluride Bi_2Te_3 and its related compounds have been the state-of-the-art thermoelectric materials at around 300 K since 1950s with a ZT value as high as 1.4 in nanocrystalline bulk specimen.^{1,6,7)} The electronic structure of Bi_2Te_3 is characterized by highly anisotropic and degenerated energy band, which is believed to be origin of good thermoelectric performance.⁸⁾ On the other hand, compared to tellurides and selenides, little attention has been paid for thermoelectric properties of bismuth-based sulfides because of their poor ZT value, except for few reports.^{9,10)} However, recent studies on sulfide systems have clearly shown that sulfides also exhibit attractive thermoelectric properties.^{11,12)} Beside thermoelectricity, superconductivity of layered bismuth sulfides, such as $\text{Bi}_4\text{S}_3\text{O}_4$,²⁾ $\text{ReBiS}_2\text{O}_{1-x}\text{F}_x$ ($\text{Re} = \text{La}, \text{Ce}, \text{Pr}, \text{Nd}, \text{and Yb}$),¹³⁻¹⁹⁾ and $\text{Ae}_{1-x}\text{Re}_x\text{BiS}_2\text{O}$ ($\text{Ae} = \text{Sr and Eu}$),²⁰⁻²³⁾ has invented the novel avenue for researches of superconductivity (the chemical formula is

written according to standard nomenclature²⁴⁾). The crystallographic structures of these compounds are basically composed of alternate stacks of BiS₂ layer and oxide/fluoride layer, as shown in the inset of Fig. 1. The conduction band near the Fermi level is primarily composed of in-plane Bi 6*p* orbitals. The thermoelectric properties of LaBiS₂O are reduced by F-substitution,²⁶⁾ whereas it is increased by Se-substitution.²⁷⁾ Recently, EuBiS₂F was reported as a possible compound that exhibits charge-density-wave-like order below 280 K and superconductivity below 0.3 K without element substitution.²³⁾ Formal valence of Eu is described as ~2.2, resulting in self electron doping to the BiS₂ conduction layer. Specific heat measurement showed the significant hybridization between Eu 4*f* and Bi 6*p* electrons, while density functional theory (DFT) calculation indicates that valence band maximum consists of Eu 4*f* orbitals.²³⁾ Given the fact of previous study, it was controversial from the viewpoint of thermoelectricity, whether Eu 4*f* and Bi 6*p* hybridized orbitals are effective to modulate Fermi surface and enhance *S*,²⁸⁾ or reduce *S* due to coexistence of electron and hole, *i.e.*, mixed conduction. In this study, we demonstrate the electrical and thermal transport of EuBiS₂F at temperatures between 300 and 623 K. Despite significant hybridization between Eu 4*f* and Bi 6*p* electrons, the charged carrier transport of EuBiS₂F is similar to that of F-doped LaBiS₂O, indicating that the EuF layer primarily act as a charge reservoir, at least above 300 K.

Polycrystalline EuBiS₂F was prepared by the solid-state reaction using EuS (99.9%), BiF₃ (99.9%), and Bi₂S₃ as starting materials. Bi₂S₃ was obtained by the solid-state reaction of Bi (99.999%) and S (99.99%) heated at 800 °C in a sealed silica tube. Then, stoichiometric mixture of starting materials was pelletized and heated at 780 °C for 20 h. The obtained sample was ground, pelletized, sealed into a silica tube and heated under the same heating conditions for homogenization. The relative density of the sample was calculated to be 90%. The purity of sample was examined using X-ray diffraction (XRD) collected using CuKα radiation (Rigaku RINT 2500). The reference grade Si (NIST RM640d) was utilized as external reference standard. Rietveld analysis was performed using the RIETAN-FP code.²⁹⁾

The Hall coefficient (R_H) at room temperature was measured using the four-probe geometry under magnetic fields (H) up to $\mu_0 H = \pm 1$ Tesla. The Hall carrier concentration (n_H) was calculated as $n_H = 1/R_H e$, where e is the charge of an electron. The measurements of ρ , S , and κ were conducted between room temperature and about 623 K using a lamp heating unit (Ulvac, MILA-5000). The value of ρ was measured by the dc four-probe technique. S was obtained from the slopes of the plots of the Seebeck voltages vs. temperature differences (ΔT) measured with Pt–Pt/Rh 13% thermocouples. The value of κ was obtained from the slopes of

the plots of heat flux density vs. ΔT . The heat loss by radiation through the sample was subtracted under the assumption that emissivity is independent of temperature and wavelength during the measurements of κ . The emissivity was evaluated on the basis of reflectivity measurements, which was performed using a spectrometer equipped with an integrating sphere (Hitachi High-tech, U-4100). The uncertainty of the κ measurements was estimated to be 10%.³⁰⁾ Measurements of electrical and thermal transport were performed in the same direction of the polycrystalline sample.

Figure 1 shows the XRD pattern of the sample and the results of Rietveld refinement. Almost all diffraction peaks corresponded to those of the EuBiS_2F phase, indicating that this phase was dominant in the samples. Although diffraction peaks due to unknown impurities were also observed, diffraction intensities of the impurity phases relative to those of EuBiS_2F were $\sim 1\%$, suggesting the amount of impurities was at these levels in the sample. The bond valence sum (BVS) of Eu was calculated to be 2.16(1) using following BVS parameters: $b_0 = 37$ pm for all atoms, $R_0 = 204$ pm and 253 pm for Eu–F and Eu–S bonds, respectively.³¹⁾ This mixed valence state of Eu is consistent with previously reported value, indicating self electron doping into the conduction layer. The negative polarity of R_H at 300 K confirms that dominant carrier is an electron at this temperature. The n_H was calculated to be $3.2(2) \times 10^{21} \text{ cm}^{-3}$ assuming single band model.

Figure 2 shows the electrical and thermal transport properties versus temperature of EuBiS_2F . The value of ρ is 3.9 m Ωcm at 300 K and it slightly decreases with increasing temperature, as shown in Fig. 2(a). On the other hand, Zhai *et al.* reported the ρ of ~ 2.2 m Ωcm at 300 K with positive temperature coefficient ($d\rho/dT$) between 300 and 350 K.²³⁾ This different ρ – T plot is probably due to self-doping owing to mixed valence of Eu and/or inevitable Bi off-stoichiometry, which is previously examined using X-ray diffraction³²⁾ and scanning tunneling microscope.³³⁾ It should be noted that electrical transport of layered oxysulfide LaCuSO , which belongs to similar crystal structure to EuBiS_2F , is extremely sensitive to Cu off-stoichiometry.³⁴⁾

Figure 2(b) shows the S as a function of temperature. The absolute value of S is $\sim 32 \mu\text{VK}^{-1}$ and it increases almost linearly up to 623 K. Both ρ – T and S – T plot is similar to that of $\text{LaBiS}_2\text{O}_{1-x}\text{F}_x$ ($x \approx 0.5$),²⁶⁾ suggesting that the charged carrier transport of EuBiS_2F at these temperatures is primarily determined by carrier concentration provided by oxide/fluoride layer, not by hybridization between Eu $4f$ and Bi $6p$ electrons.

Figure 2(c) shows the total thermal conductivity (κ_{tot}) versus temperature. The lattice

thermal conductivity (κ_l) was calculated by subtracting electronic thermal conductivity (κ_{el}) from κ_{tot} . The κ_{el} was obtained by Wiedemann–Franz relation, $\kappa_{el} = LT\rho^{-1}$, where L is the Lorenz number, $L = 2.45 \times 10^{-8} \text{ W}\Omega\text{K}^{-2}$. The value of κ_l was 1.5–2.0 $\text{Wm}^{-1}\text{K}^{-1}$ at temperatures between 300 and 623 K. This value is distinctly lower than that of isostructural SrBiS_2F ($\kappa_l \approx 2.7 \text{ Wm}^{-1}\text{K}^{-1}$),³⁵⁾ while it is similar to that of LaBiS_2O ($\kappa_l \approx 2.0 \text{ Wm}^{-1}\text{K}^{-1}$),²⁷⁾ which is attributed to lower speed of sound resulted from heavier atomic mass of Eu ion.³⁶⁾ Notably, relative density of the sample in this study is 90%. According to the effective medium theory (EMT) by Maxwell-Garnett, a 14% reduction in κ is expected from the sample with 90% of relative density under the assumption that 10% of pores are randomly distributed and separated sphere.³⁷⁻⁴⁰⁾ Fully dense sample will be required to elucidate the detailed thermal transport mechanism of these compounds. Furthermore, the EMT predicts an increase of 16% in ρ of the sample with 90% of relative density. The dimensionless figure of merit is calculated to be 0.02 at 623 K.

We briefly discuss the possible way that may improve the ZT of these compounds. A typical way to enhance the ZT is tuning the n_H . The ZT of state-of-the-art thermoelectric materials, such as Bi_2Te_3 and PbTe , is optimized at the n_H of 10^{19} – 10^{20} cm^{-3} ,⁵⁾ while the n_H of EuBiS_2F is $3.2(2) \times 10^{21} \text{ cm}^{-3}$, as described above. However, the ZT of LaBiS_2O , which has the n_H of $\sim 10^{19} \text{ cm}^{-3}$,⁴¹⁾ is in the same order with that of EuBiS_2F ,²⁷⁾ suggesting that simply tuning the n_H is not attractive way to improve the ZT of these compounds. Band engineering is more reasonable way to improve the ZT , as demonstrated by Se-substitution in LaBiS_2O .²⁷⁾ Notably, detailed mechanism of an enhancement of ZT in Se-doped LaBiS_2O is not clarified yet. Density functional theory calculation is believed to be effective to shed light on the issue as well as the measurements of transport properties of fully dense samples. Another strategy to enhance the ZT is reducing thermal conductivity. For example, the lattice thermal conductivity of layered oxychalcogenide LaCuSeO was reported as $2.1 \text{ Wm}^{-1}\text{K}^{-1}$ at 300 K,⁴²⁾ while that of BiCuSeO was $< 1.0 \text{ Wm}^{-1}\text{K}^{-1}$,⁴³⁾ indicating thermal conductivity of these layered compounds can be reduced by substitution for oxide layer. Actually, the lattice thermal conductivity of EuBiS_2F is distinctly lower than that of isostructural SrBiS_2F , which confirms the possibility of reducing lattice thermal conductivity of these compounds by element substitution.

In summary, we demonstrate the electrical and thermal transport of layered bismuth-based sulfide EuBiS_2F at temperatures between 300 and 623 K. Although significant hybridization between Eu $4f$ and Bi $6p$ electrons was previously reported, the charged carrier transport of EuBiS_2F is similar to that of F-doped LaBiS_2O , at least above 300 K. These results strongly

suggest that electron doping into BiS_2 layer is detrimental for thermoelectric properties of layered bismuth-chalcogenides. The κ_1 is distinctly lower than that of isostructural SrBiS_2F , which is probably due to heavier atomic mass of Eu ions.

Figure captions

Fig. 1.

(Color online) X-ray diffraction pattern of EuBiS_2F and the results of Rietveld analysis. Crosses (red) and solid line (red) represent observed and calculated patterns, respectively. The difference between the observed and calculated patterns is shown at the bottom (black). The vertical marks (black) indicate the Bragg diffraction angles of EuBiS_2F . The arrows denote the diffraction peaks due to unknown impurities. The lattice parameters were calculated to be $a = 0.40488(1)$ nm and $c = 1.353240(6)$ nm. The reliability factor (R_{wp}) is 8.48%. Site occupancies of each sites are fixed at unity. The inset shows the crystallographic structure of EuBiS_2F , which is depicted using VESTA software.²⁵⁾

Fig. 2.

(Color online) Electrical and thermal transport properties versus temperature (T) of EuBiS_2F . (a) Electrical resistivity (ρ), (b) Seebeck coefficient (S), and (c) thermal conductivity (κ). The lattice thermal conductivity (κ_l) was calculated by subtracting electronic thermal conductivity from total thermal conductivity (κ_{tot}).

Acknowledgment

This work was partially supported by research grants from Keio University, the Keio Leading-edge Laboratory of Science and Technology (KLL), Japan Society for Promotion of Science (JSPS) KAKENHI Grant Number 25707031 and 26400337, and the Asahi Glass Foundation.

*E-mail: matobam@appi.keio.ac.jp

†Present address: Department of Chemical System Engineering, School of Engineering, The University of Tokyo, Hongo 113-8656, Japan

References

- 1) H. J. Goldsmid and R. W. Douglas, *Br. J. Appl. Phys.* **5**, 386 (1954).
- 2) Y. Mizuguchi, H. Fujihisa, Y. Gotoh, K. Suzuki, H. Usui, K. Kuroki, S. Demura, Y. Takano, H. Izawa, and O. Miura, *Phys. Rev. B* **86**, 220510 (2012).
- 3) A. Kudo, K. Omori, and H. Kato, *J. Am. Chem. Soc.* **121**, 11459 (1999).
- 4) J. Wang, J. B. Neaton, H. Zheng, V. Nagarajan, S. B. Ogale, B. Liu, D. Viehland, V. Vaithyanathan, D. G. Schlom, U. V. Waghmare, N. A. Spaldin, K. M. Rabe, M. Wuttig, and R. Ramesh, *Science* **299**, 1719 (2003).
- 5) G. J. Snyder and E. S. Toberer, *Nat. Mater.* **7**, 105 (2008).
- 6) D. Y. Chung, T. Hogan, P. Brazis, M. Rocci-Lane, C. Kannewurf, M. Mastea, C. Uher, and M. G. Kanatzidis, *Science* **287**, 1024 (2000).
- 7) B. Poudel, Q. Hao, Y. Ma, Y. Lan, A. Minnich, B. Yu, X. Yan, D. Wang, A. Muto, D. Vashaee, X. Chen, J. Liu, M. S. Dresselhaus, G. Chen, and Z. Ren, *Science* **320**, 634 (2008).
- 8) P. Larson, S. D. Mahanti, and M. G. Kanatzidis, *Phys. Rev. B* **61**, 8162 (2000).
- 9) H. Mizoguchi, H. Hosono, N. Ueda, and H. Kawazoe, *J. Appl. Phys.* **78**, 1376 (1995).
- 10) B. Chen, C. Uher, L. Iordanidis, and M. G. Kanatzidis, *Chem. Mater* **9**, 1655 (1997).
- 11) K. Suekuni, K. Tsuruta, M. Kunii, H. Nishiate, E. Nishibori, S. Maki, M. Ohta, A. Yamamoto, and M. Koyano, *J. Appl. Phys.* **113**, 043712 (2013).
- 12) Y. He, T. Day, T. Zhang, H. Liu, X. Shi, L. Chen, and G. J. Snyder, *Adv. Mater.* **26**, 3974 (2014).
- 13) Y. Mizuguchi, S. Demura, K. Deguchi, Y. Takano, H. Fujihisa, Y. Gotoh, H. Izawa, and O. Miura, *J. Phys. Soc. Jpn* **81**, 114725 (2012).
- 14) S. Demura, Y. Mizuguchi, K. Deguchi, H. Okazaki, H. Hara, T. Watanabe, S. J. Denholme, M. Fujioka, T. Ozaki, H. Fujihisa, Y. Gotoh, O. Miura, T. Yamaguchi, H. Takeya, and Y. Takano, *J. Phys. Soc. Jpn.* **82**, 033708 (2013).
- 15) J. Xing, S. Li, X. Ding, H. Yang, and H. H. Wen, *Phys. Rev. B* **86**, 214518 (2012).
- 16) R. Jha, A. Kumar, S. K. Singh, and V. P. S. Awana, *J. Sup. Novel Mag.* **26**, 499 (2013).
- 17) D. Yazici, K. Huang, B. D. White, A. H. Chang, A. J. Friedman, and M. B. Maple, *Philos. Mag.* **93**, 673 (2013).
- 18) K. Deguchi, Y. Mizuguchi, S. Demura, H. Hara, T. Watanabe, S. J. Denholme, M. Fujioka,

- H. Okazaki, T. Ozaki, H. Takeya, T. Yamaguchi, O. Miura, and Y. Takano, *EPL* **101**, 17004 (2013).
- 19) D. Yazici, K. Huang, B. D. White, I. Jeon, V. W. Burnett, A. J. Friedman, I. K. Lum, M. Nallaiyan, S. Spagna, and M. B. Maple, *Phys. Rev. B* **87**, 174512 (2013).
- 20) X. Lin, X. Ni, B. Chen, X. Xu, X. Yang, J. Dai, Y. Li, X. Yang, Y. Luo, Q. Tao, G. Cao, and Z. Xu, *Phys. Rev. B* **87**, 020504 (2013).
- 21) H. Sakai, D. Kotajima, K. Saito, H. Wadati, Y. Wakisaka, M. Mizumaki, K. Nitta, Y. Tokura, and S. Ishiwata, *J. Phys. Soc. Jpn.* **83**, 014709 (2014).
- 22) R. Jha, B. Tiwari, and V. P. S. Awana, *J. Appl. Phys.* **117**, 013901 (2015)
- 23) H. F. Zhai, Z. T. Tang, H. Jiang, K. Xu, K. Zhang, P. Zhang, J. K. Bao, Y. L. Sun, W. H. Jiao, I. Nowik, I. Felner, Y. K. Li, X. F. Xu, Q. Tao, C. M. Feng, Z. A. Xu, and G. H. Cao, *Phys. Rev. B* **90**, 064518 (2014).
- 24) Z. Hiroi, e-print arXiv:0805.4668.
- 25) K. Momma and F. Izumi, *J. Appl. Crystallogr.* **44**, 1272 (2011).
- 26) A. Omachi, J. Kajitani, T. Hiroi, O. Miura, and Y. Mizuguchi, *J. Appl. Phys.* **115**, 083909 (2014).
- 27) Y. Mizuguchi, A. Omachi, Y. Goto, Y. Kamihara, M. Matoba, T. Hiroi, J. Kajitani, and O. Miura, *J. Appl. Phys.* **116**, 163915 (2014).
- 28) A. Benti, S. Johnsen, G. K. H. Madsen, B. B. Iversen, and F. Steglich, *Europhys. Lett.* **80**, 17008 (2007).
- 29) F. Izumi and K. Momma, *Solid State Phenomena* **130**, 15 (2007)
- 30) Y. Goto, Y. Sakai, Y. Kamihara, and M. Matoba, *J. Phys. Soc. Jpn.* **84**, 044706 (2015).
- 31) N. E. Brese and M. O'Keeffe, *Acta Crystallogr.* **B47**, 192 (1991).
- 32) A. Miura, M. Nagao, T. Takei, S. Watauchi, and I. Tanaka, *J. Solid State Chem.* **212**, 213 (2014).
- 33) T. Machida, Y. Fujisawa, M. Nagao, S. Demura, K. Deguchi, Y. Mizuguchi, Y. Takano, and H. Sakata, *J. Phys. Soc. Jpn.* **83**, 113701 (2014).
- 34) Y. Goto, M. Tanaki, Y. Okusa, T. Shibuya, K. Yasuoka, M. Matoba, and Y. Kamihara, *Appl. Phys. Lett.* **105**, 022104 (2014).
- 35) H. Lei, K. Wang, M. Abeykoon, E. S. Bozin, and C. Petrovic, *Inorg. Chem.* **52**, 10685 (2013).
- 36) E. S. Toberer, A. Zevkink, and G. J. Snyder, *J. Mater. Chem.* **21**, 15843 (2011).
- 37) J. C. Maxwell-Garnett, *Philos. Trans. R. Soc. London Ser. A* **203**, 385 (1904).
- 38) K. W. Schlichting, N. P. Padture, and P. G. Klemens, *J. Mater. Sci.* **36**, 3003 (2001).

- 39) Y. Zhang, T. Day, M. L. Snedaker, H. Wang, S. Krämer, C. S. Birkel, X. Ji, D. Liu, G. J. Snyder, and G. D. Stucky, *Adv. Mater.* **24**, 5065 (2012).
- 40) In the effective medium theory by Maxwell-Garnett, the effective dielectric constant (ϵ_{eff}) of the medium consists of matrix medium and inclusions are expressed as follows,
$$\epsilon_{\text{eff}} = \epsilon_m \frac{2(1 - \delta_i)\epsilon_m + (1 + \delta_i)\epsilon_i}{(2 + \delta_i)\epsilon_m + (1 - \delta_i)\epsilon_i}$$
, where ϵ_m , ϵ_i , and δ_i are the dielectric constant of the matrix, the dielectric constant of the inclusion, and the volume fraction of the pores, respectively.
- 41) I. Pallecchi, G. Lamura, M. Putti, J. Kajitani, Y. Mizuguchi, O. Miura, S. Demura, K. Deguchi, and Y. Takano, *Phys. Rev. B* **89**, 214513 (2014).
- 42) M. Yasukawa, K. Ueda, and H. Hosono, *J. Appl. Phys.* **95**, 3594 (2004).
- 43) L. D. Zhao, D. Berardan, Y. L. Pei, C. Byl, L. Pinsard-Gaudart, and N. Dragoë, *Appl. Phys. Lett.* **97**, 092118 (2010).

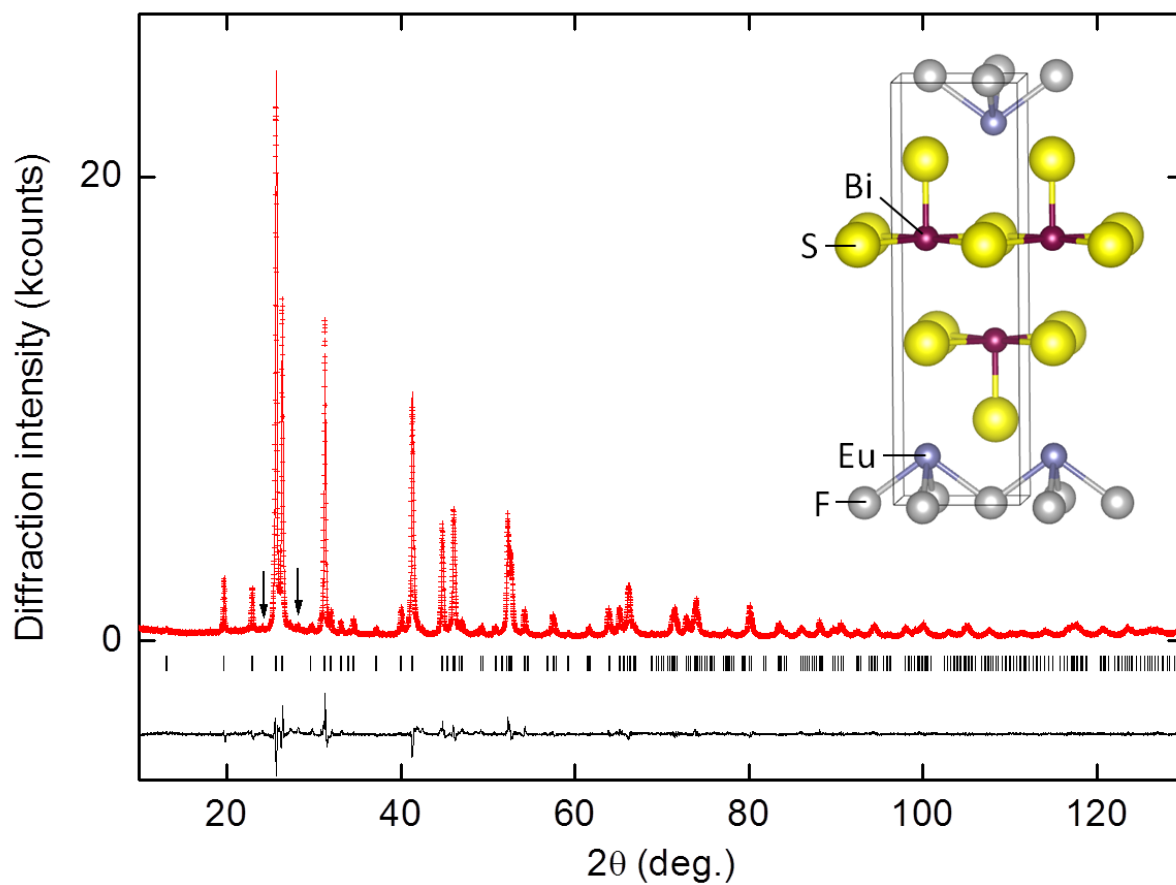


Fig. 1. (Color online)

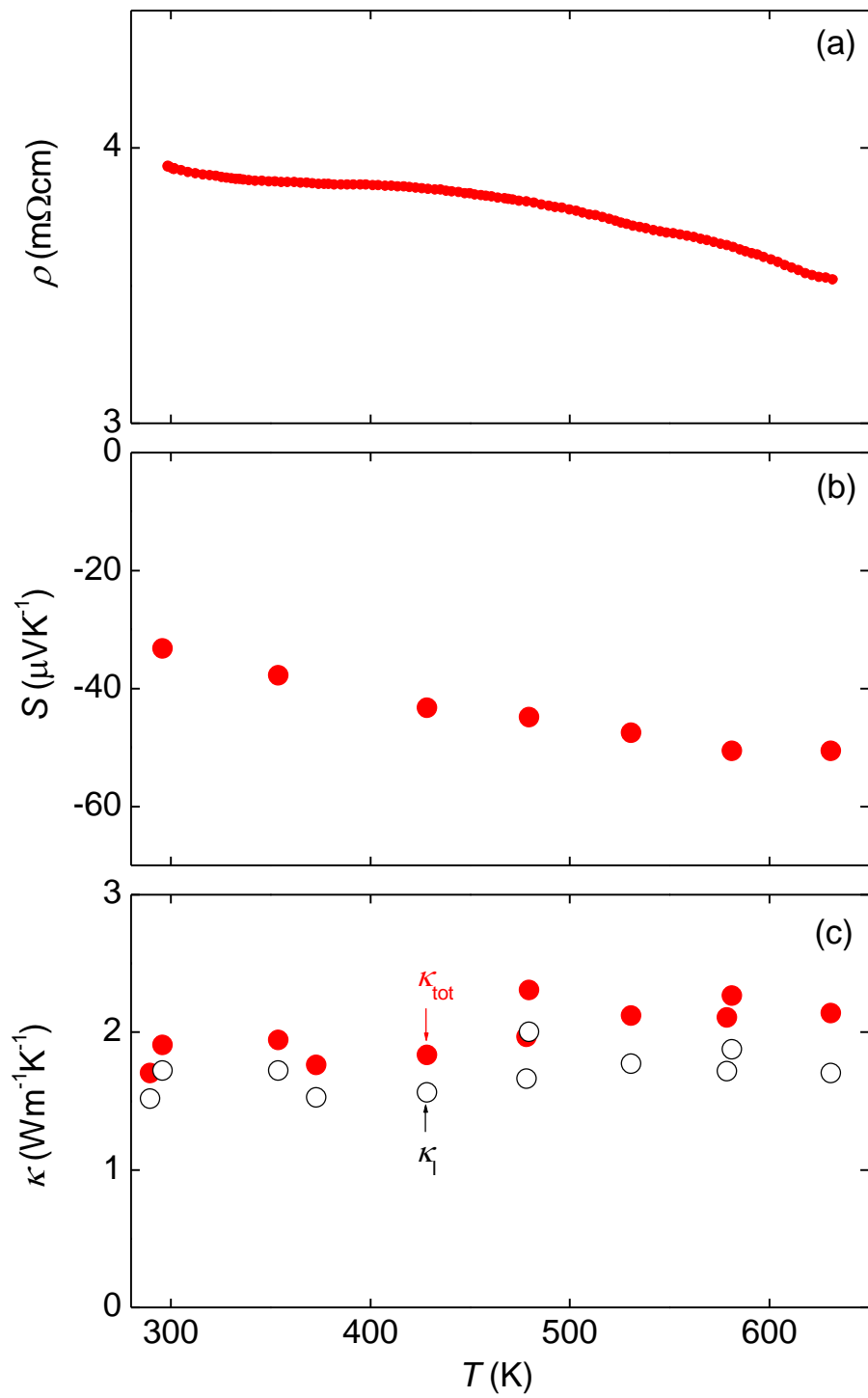


Fig. 2. (Color online)